

Experiments for two-phase pressure drop in flooded packed bed at high air velocity

Mooneon Lee^a, Hyun Sun Park^{a*}, Jin Ho Park^a, Kiyofumi Moriyama^a, Moo Hwan Kim^a
*a Division of Advanced Nuclear Engineering, Pohang university of science and technology (POSTECH)
San 31, Hyoja-dong, Nam-gu, Pohang, Gyungbuk, Republic of Korea, 37673*
**Corresponding author: hejsunny@postech.ac.kr*

1. Introduction

If a severe core degradation arises and is relocated to a pre-flooded reactor cavity in a light water reactor (LWR), the ex-vessel debris bed may be formed with settled corium particles rather than molten phase due to FCI (Fuel Coolant Interaction). Therefore, the cooling limitation of particulate debris bed has to be reliably assessed for analyzing its possibility of re-melting that may lead to MCCI (Molten Core Concrete Interaction) threatening containment integrity.

One of the key parameters to represent the debris bed cooling limit is the Dryout Heat Flux (DHF), defined as the maximum heat flux through the bed without dryout. One of the dominant phenomenological factors of dryout occurrence is the flow resistance in the packed particles. Therefore, many researches[1-6] have attempted to model the two-phase friction terms to predict DHF precisely. Various previous models[2, 3, 5, 6] show relatively good agreement with DHF experimental data conducted with a 1D top flooding condition[7]. On the other hand, most of those models encounter to difficulties of predicting DHF at the co-current flow conditions[6] expected to be observed in ex-vessel debris bed with lateral water ingress. Some models are, however, able to precisely predict DHF results at the co-current conditions, while tending to underestimate the pressure gradient. Therefore, none of models are able to predict both DHF and pressure drop in the packed bed so far.

In our previous work[8], the cause of disagreement between experimental data and previously suggested models were analyzed. From the analysis, it is found that the most pressure drop experiments in literature were validated with pressure drop experiment up to relatively moderate void fraction (~ 0.6), while a recent pressure drop experiment[9] conducted at 2 mm and 3.5 mm implies the sudden increase of interfacial friction at high void fraction condition ($0.6 < \alpha < 1$). Based on the experimental observation, we proposed a new model that shows the potential capability to predict both DHF and pressure drop at the same time.

The aim of this work is to gather experimental data base on two-phase flow pressure drop at high void fraction range to extend capability of model into wider range of particle sizes which will be used to predict DHF of ex-vessel debris bed.

2. Methods and Results

2.1 PICASSO Facility

The two-phase pressure drop experimental facility, named as PICASSO (Pressure drop Investigation and Coolability ASSESSment through Observation) illustrated in Fig.1., is used in this work. The PICASSO facility consists of the test section, pressure differential transducer and air flow switch.

The test section is fabricated of an acrylic tube with the inner diameter of 100 mm and the height of 700 mm. The pressure ports are drilled on the side wall of the test section at the heights of 100 and 600 mm. The manufactured acrylic air distributor is installed at the bottom of the test section to hold particle bed and distribute air flow uniformly through bed.

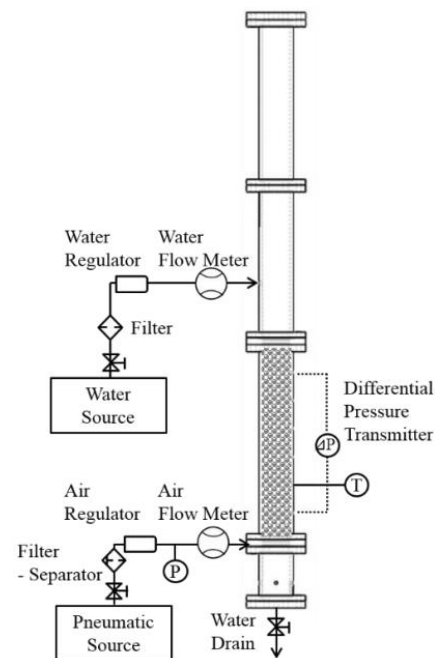


Fig. 1. Schematic of the experimental facility[10].

The air flow rate was measured by the calibrated PFMB series manufactured by SMC (2~200 LPM, 5~500 LPM and 10~1000 LPM) with the accuracy of $\pm 3\%$ at full span. The pressure difference between two pressure ports was measured by the Rosemount 3051S series ($-62.3 \sim 62.3$ kPa) with accuracy of $\pm 0.025\%$ at full span.

2.2 Experimental procedure

Before the experiment, the total mass of particles in the test section was measured to obtain the porosity of the bed. The particles with the diameter of 4.05 mm are packed in the test section and provides the porosity of 0.40 and the pressure impulse lines and the test section are filled with either air or water single-phase fluid depending on the experimental condition (the air phase at air single-phase experiment and the water phase at air/water two-phase experiment, respectively). Finally, the upward air is injected from the bottom of the bed.

All experimental data except the test at the flow velocity of 0.8 m/s was measured twice for repeatability. The exception was made due to its exceedingly long time to reach the steady state condition which is explained in the Section 2.4.

2.3 Post processing of experimental data

In the analysis, the pressure gradient in the packed bed is normalized by the hydrostatic pressure represented as a non-dimensional form defined as

$$P^* = (-dP/dz) / (\rho_l g) \quad (1)$$

where $\rho_l g$ is the hydrostatic pressure.

In the experiment, the amplitude of measurement data is sometime exceeding the measurement accuracy. Therefore, the magnitude of fluctuation is also considered in the uncertainty analysis as the standard deviation of measured data is used for random error (e_r). The systematic error, e_s , is obtained by manufacturer's specification. The uncertainty of the measured velocity and pressure difference is calculated by the equation (2) with 95% of confidence.

$$e = \sqrt{e_r^2 + e_s^2} \quad (2)$$

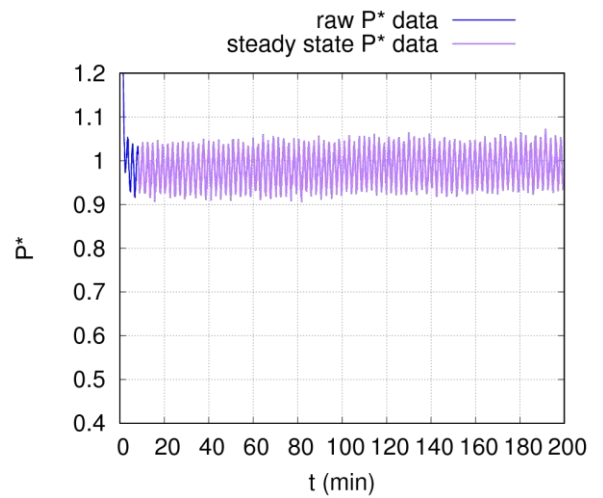
In some experiment cases, the times to reach steady state condition exponentially increase at high air velocity region before the air single phase flow formation in the test section. In order to analyze the characteristic time to reach steady-state condition (Δt_{ss}), it is defined as the time when the pressure gradient starts to be within the range of $E(\nabla P_{ss}) \pm 0.25\sigma(\nabla P_{ss})$, where the $E(\nabla P_{ss})$ is the average value of a pressure gradient at steady-state condition and $\sigma(\nabla P_{ss})$ is the standard deviation of a pressure gradient at the steady-state condition for the last 6 minutes of experiments.

2.4 Characteristic time to reach steady-state condition (Δt_{ss})

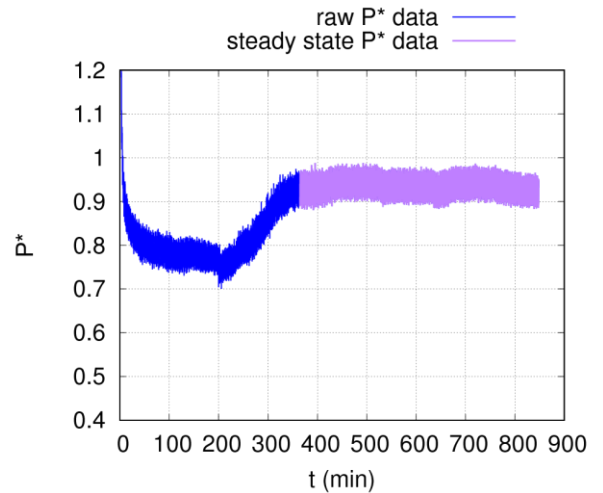
At the relatively low and moderate air velocity range (0~0.6 m/s), the system reaches the steady-state condition within 10 minutes. On the other hand, as the

air velocity increases, the time to reach the steady-state condition takes several hours. The trend of pressure gradients during experiment until the steady-state condition with different velocities are shown in Fig. 2.

In order to analyze the trend of Δt_{ss} increase at the high velocity region, Δt_{ss} is plotted with respect to the superficial air velocity as shown in Fig. 3. Δt_{ss} starts exponentially increasing at the superficial velocity above approximately 0.6 m/s. In the experimental cases with the high superficial velocity, almost no water flow channel was visually observed when the trend is at decrease. While the formation of water flow channels is clearly observed at a certain location after it reaches to steady-state condition.



(a) Pressure gradient data at 0.6 m/s



(b) Pressure gradient data at 0.78 m/s

Fig. 2. The measured pressure gradient data

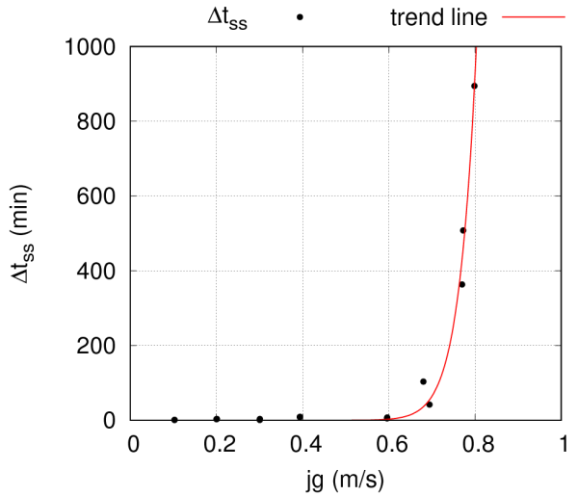


Fig. 3. The trend of Δt_{ss} increase

2.5 Two-phase flow pressure gradient

The measured pressure gradient data is plotted in Fig. 4. The abbreviation TPF and SS state Two-Phase Flow and Steady State condition, respectively.

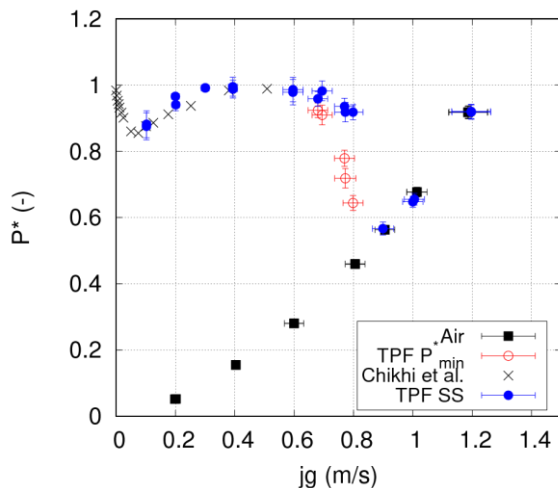


Fig. 4. Measured two-phase pressure gradient

At the low and moderate air velocity region, where Δt_{ss} stays within 10 minutes, the measured pressure gradients fits well with the experimental data in literature [11] conducted with 4 mm glass beads. The pressure gradient decreases at the low velocity region and increases up to hydrostatic head at the moderate velocity region. At the stagnant water condition, the difference between the hydrostatic head and the pressure gradient in test section is proportional to the interfacial friction force[12] as written in Eq. (3). Therefore, the increase of pressure gradient can be analyzed as the interfacial friction decreases with the air velocity increase from 0.1 to 0.6 m/s. In the previous researches, this is explained as the channel-like flow formulation which diminishes the interfacial area between air and water.

$$F_i = -\varepsilon(1-\alpha)(-\nabla P_i - \rho_i g) \quad (3)$$

On the other hand, at the high air velocity region between 0.7 and 0.8 m/s, where Δt_{ss} exponentially increases, the pressure gradient slightly decreases again at the steady-state condition. Before their steady-state condition, the pressure gradients decrease closely to the value obtained at the single phase flow. The visual observation during the experiment also confirms the single phase flow formation as mentioned in the section 2.4.

At the higher air velocity, the pressure gradient measured at two-phase flow condition reaches to the pressure gradient measured air single phase flow. At this point, no water was visually observed.

3. Conclusions

The two-phase pressure drop experiment in the spherical particles (\emptyset 4.05 mm) packed bed with stagnant water is conducted from with the air superficial velocities ranged from 0 to 1.2 m/s of air superficial velocity. The trend of data is suddenly changed when the air velocity exceeds 0.6 m/s. Below 0.6m/s, the measured pressure gradients show good agreement to the preceding research and the characteristic time to reach the steady state condition (Δt_{ss}) is less than 10 minutes. On the other hand, above 0.6 m/s of air velocity, the Δt_{ss} increases exponentially and the pressure gradient start to decrease. In the end, over 0.9 m/s of air velocity, the water phase does not exist in the test section as can be confirmed by its pressure gradient value and visual observation during the experiment.

Acknowledgements

This work was supported by the Nuclear Safety Research Program through the Korea Foundation Of Nuclear Safety(KOFONS), granted financial resource from the Nuclear Safety and Security Commission(NSSC), Republic of Korea (No. 1305008)

REFERENCES

- [1] Lipinski, R.J., A review of debris coolability models, in Light water reactor severe accident evaluation. 1983, Sandia National Labs.
- [2] Reed, A.W., The effect of channeling on the dryout of heated particulate beds immersed in a liquid pool. 1982, Ph.D thesis, Massachusetts Institute of Technology.
- [3] Schulenberg, T. and U. Müller, An improved model for two-phase flow through beds of coarse particles. International journal of multiphase flow, 1987. 13(1): p. 87-97.

- [4] Tung, V. and V. Dhir, A hydrodynamic model for two-phase flow through porous media. *International journal of multiphase flow*, 1988. 14(1): p. 47-65.
- [5] Schmidt, W., Interfacial drag of two-phase flow in porous media. *International journal of multiphase flow*, 2007. 33(6): p. 638-657.
- [6] Rahman, S., Coolability of corium debris under severe accident conditions in light water reactors, 2013, Ph.D thesis, Universität Stuttgart.
- [7] Lee, M., et al., Comparison of Two Phase Pressure Drop Models in 1-D Top Flooded Debris Bed, in *Transactions of the Korean Nuclear Society Spring Meeting*, 2016: Jeju.
- [8] Lee, M., et al., Comparison of Dryout Heat Flux Models in One Dimensional Porous Bed Configuration, in *NURETH-17*. 2017: Xian, China.
- [9] Park, J.H., et al., Effect of particle shape on pressure gradients of water/air two-phase flow in the particulate beds for ex-vessel coolability, in *ICAPP 2016*. 2016: San Fransisco, CA.
- [10] Park, J.H., et al., Influence of Spherical Particle Size Distribution on Pressure Gradients in Mixed Bed. 2016.
- [11] Chikhi, N., et al., Pressure drop and average void fraction measurements for two-phase flow through highly permeable porous media. *Annals of Nuclear Energy*, 2016. 94: p. 422-432.
- [12] Li, L., et al., Pressure losses and interfacial drag for two-phase flow in porous beds with coarse particles. *Annals of Nuclear Energy*, 2017. 101: p. 481-488.